Received: 11 January 2019 | Revised: 25 February 2019 | Accepted: 17 March 2019 | Published on: 17 June 2019

DOI: 10.1002/ctpp.201900005

ORIGINAL ARTICLE

Contributions to Plasma Physics

Radar studies of ionospheric dusty plasma phenomena

I. Mann[1] | T. Gunnarsdottir[1] | I. Häggström[2] | S. Eren[1] | A. Tjulin[2] | M. Myrvang[1] | M. Rietveld[3] | P. Dalin[4] | D. Jozwicki[1] | H. Trollvik[1]

[1]Department of Physics and Technology, UIT—The Arctic University of Norway, Tromsø, Norway

[2]EISCAT Scientific Association, EISCAT, Kiruna, Sweden

[3]EISCAT Norway, UIT—The Arctic University of Norway, Tromsø, Norway

[4]Swedish Institute of Space Physics, Kiruna, Sweden

Correspondence
Ingrid Mann, Department of Physics and Technology, UIT—The Arctic University of Norway, 6050 Tromsø 9037, Norway.
Email: ingrid.b.mann@uit.no

Funding information
Norges Forskningsråd, NFR 275503

We discuss the influence of charged dust on radar observations in the Earth ionosphere. This region in the upper Earth atmosphere can be described as a partially ionized, low-temperature plasma. Plasma parameters vary by orders of magnitude spatially and in time. Dust particles influence the charge balance, in some cases dusty plasma condition is met. The polar mesospheric echoes are an example of dust plasma interactions observed with radar. The mesosphere is a region where atmospheric temperature decreases with altitude and can reach frost point temperature. The formation of the polar mesospheric radar echoes involves neutral atmosphere dynamics, which is latitude dependent and it involves charged dust particles, especially icy dust that forms in the polar summer mesosphere. Charged dust can also influence incoherent scatter that results from electromagnetic waves scattering off electrons, where the electrons are coupled to other charged components. Observers rarely report charged dust signatures in the incoherent scatter spectra; we show that there is a good chance for doing so with improved observations. The incoherent scatter can possibly also be used to estimate the amount of charged dust in the direct vicinity of a meteor, as we show based on the order of magnitude considerations. This prospect of new observational results makes theoretical investigations of radio-wave scattering in the presence of charged dust with size distributions worthwhile.

KEYWORDS
dusty plasma, incoherent scatter, ionospheric physics, nanoparticles, radar observations

1 | INTRODUCTION

Scattering of electromagnetic waves in plasma provides a tool of remote diagnostics and is used in laboratory and fusion plasmas. It is also used to study the partly ionized gas of the upper Earth atmosphere,[1] where because of the scaling of wavelength and Debye length (Figure 1) the characteristic scattering occurs for radio waves and is observed with radar. This process, which for historical reasons is called incoherent scatter, is used to probe the upper atmosphere typically from 100 to 600 km and with advanced instruments and analysing techniques further can also be used this region can extend above and below. The incoherent scatter can also be influenced by the charged dust particles, a dusty plasma effect that is predicted, but so far only observed in a few cases. Dust particles exist in the meteor ablation zone and below. The amount of dust and its surface charge are important

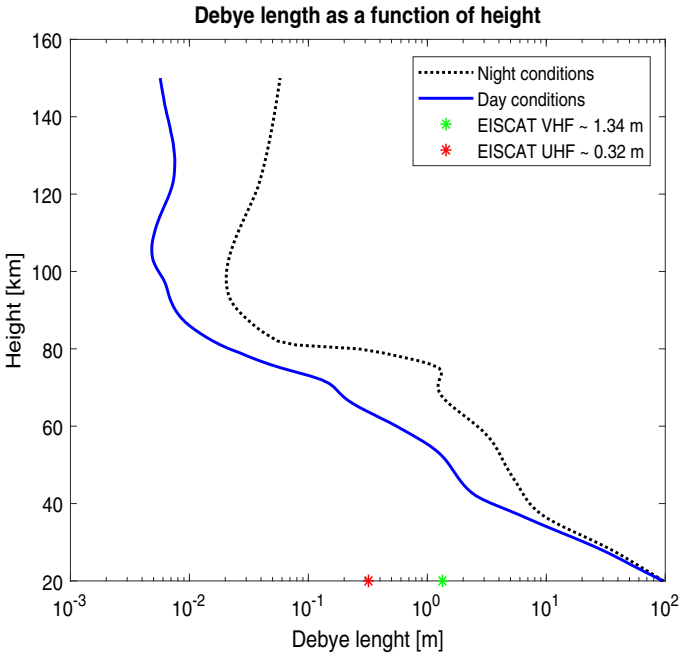

FIGURE 1 The electron Debye length in the Earth's lower ionosphere based on electron density and temperature calculated[2] for conditions at 69°N and 16°E (Andenes, Norway) on September 8, 2010 at local times 23:55 (night) and 12.15 (day). The EISCAT VHF and UHF wavelengths are marked in the abscissa

parameters in the physics and chemistry of the upper atmosphere and we discuss here the chances prospects to detect the charged dust with incoherent scatter. Radar also observe meteors that form when cosmic dust and meteoroid particles enter the atmosphere, and radar detect (coherent) strong radar echoes, that are linked or possibly linked to the presence of charged dust.

Because of the small cross section of the underlying Thomson scattering at free atmospheric electrons, observing incoherent scatter requires using high-power, large aperture radar. Such facilities that are located around the globe at a few fixed locations. This article refers to the incoherent scatter observations made with the EISCAT radars near Tromsø (VHF 224 MHz, UHF 933 MHz) and on Svalbard (ESR 500 MHz). Their locations at high latitude are interesting for ionospheric research because the plasma in the upper polar atmosphere is highly variable from day to night and influenced by the Sun–Earth interactions. The upper polar atmosphere is also interesting for climate research because during summer it reaches the globally lowest temperatures. We discuss the influence of the charged dust on incoherent scatter and other radar observations of the dust.

2 | IONOSPHERE AND ITS DUST COMPONENTS

The upper atmosphere where solar radiation determines the degree of ionization, called the ionosphere, contains atomic and molecular ions and neutrals. It is partially ionized to various degrees at its different altitudes from roughly 60 to 1,000 km and the density decreases with increasing altitude over many orders of magnitude. The plasma temperatures range from as low as 100 to 2,000 K. The Debye length varies from cm to mm scale and varies with ionospheric conditions (Figure 1). The lower ionosphere overlaps with the upper mesosphere. The mesosphere is the part of the Earth atmosphere where temperature decreases with the altitude, its boundaries vary over the year and with latitude. Its upper boundary is the region of lowest temperature. The upper mesosphere also overlaps with the meteor ablation zone (~70–130 km), where meteoroids (dust particles) that fall into the atmosphere are decelerated and ablate.[3] A large fraction of the meteoroid material diffuses into the atmosphere in solid and gaseous form. The metallic ions that are presumably of meteoric origin are observed as sporadic E-layers.[4] Dust particles with radii from a few 10 nm to less than nm form out of the material that is released during the meteoroid ablation.

The forming particles are transported in the atmospheric zonal and meridional circulation that are influenced by gravity waves.[5,6] The dust particles contribute to formation of icy particles when the temperature close to the mesopause reaches its frost point. The small dust acts as nucleation centres so the ice particles form faster than the homogenous condensation from gas phase does. Models suggest that nucleation forms icy dust of radii 10–50 nm.[7] While models[5,6] assume that initial condensates of 0.2 nm size form in the meteor plumes, there is an uncertainty about the smallest size of the dust particles. Instruments on atmospheric rockets measure the impacts of charged dust particles. The detections go down to roughly 0.5 nm radius (~500 amu).[8] This is not necessarily the lower size limit, because small particles are deflected in the airflow around the rocket and, therefore, not measured (see e.g. ref. [9]). The larger among the icy dust particles are observed in noctilucent clouds,[10,11] with optical images,[12,13] with lidar,[14] and optically from satellites.[15]

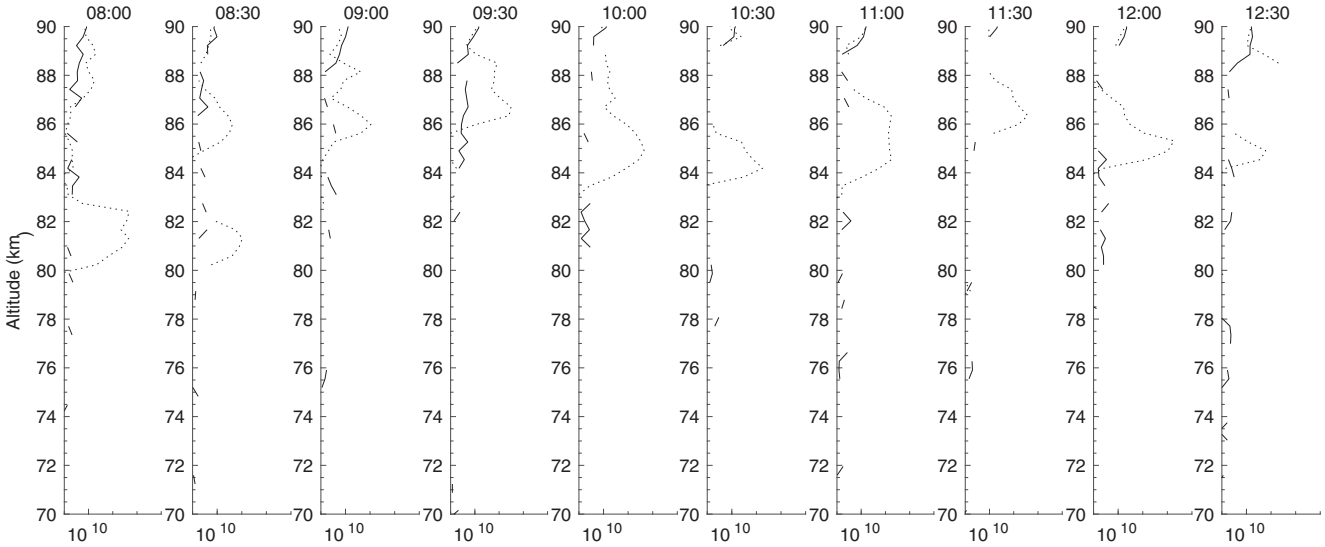

FIGURE 2 The electron density observed with EISCAT UHF (solid line, in units m^{-3}) and Polar Mesospheric Summer Echoes (PMSE, dashed line, in arbitrary units) observed with EISCAT VHF on June 26, 2013 from 7:30 and 13:00 UT. Data shown are accumulated over 30 min time^{-3}) and Polar Mesospheric Summer Echoes (PMSE, dashed line, in arbitrary units) observed with EISCAT VHF on June 26, 2013 from 7:30 and 13:00 UT. Data shown are accumulated over 30 min time intervals

Another parameter that is difficult to derive from observations is the dust charge and it is seen as a key parameter to understand the formation of mesospheric ice particles.[7,11] Through its influence on the number of free electrons, the dust charge also influences atmospheric chemistry.[4,16,17] The charged dust particles are involved in processes that are observed with radar as we discuss below.

3 | DUST CHARGING IN DETAIL

Dust particles charge by collecting and emitting electrons and ions. Impacting electrons and ions with low energy stick to the particles so that a charge builds up. Impacting high-energy particles produce secondary emission. Impacting photons can cause photo-electron emission icy or photo-detachment from negatively charged dust. All these processes generate charging currents, which at the same time vary with the dust surface charge that attracts or repels the charged particles. For moderate plasma temperatures, in the absence of solar radiation the dust particles typically reach a negative equilibrium charge. The attachment of the electrons to the dust leads to a lack of free electrons in the layers with large (icy) dust particles. This phenomenon was observed with rocket observations where the electron flux lowered when the measured dust flux was large. This so-called electron bite-out is, however, not always observed. Similarly, the bite-outs are rarely seen with radar observations. Figure 2 shows altitude profiles of observations with two co-located EISCAT radars. The EISCAT UHF detected incoherent scatter from which electron densities are derived and shown in the figure. EISCAT VHF measured coherent Polar Mesospheric Summer Echoes (PMSE) signals that form in the presence of charged dust, as we discuss below (Section 4). While the analysis of incoherent scatter from low altitude where electron densities are low bears an uncertainty (see Section 5), it is still worthwhile to note that none of the measurements shown in the figure suggest a reduced electron density at the altitude and time of the PMSE signal, i.e. in the presence of dust. This illustrates that dust charging is more complex.

In reality, the dust can also be neutral or positively charged and particles of a few nm-size have a charge of 0 or ±e only.[7,16,18,19] Even small amounts of high-energy particles change the charge balance.[20] Auroral precipitation brings ∼1–10 keV electrons to 100–120 km altitudes and those with $E > 10$ keV even deeper. They lead to secondary electron emission, which in addition is influenced by small particle effects.[19] Impacts of photons cause photo-electron emission when the photon energy is greater than the work function of the dust material. Photon impacts on negatively charged dust can lead to detachment of electrons. In addition to solar photon flux, ionospheric processes (e.g. aurora) and geo-corona can possibly influence the charging and the dust light scattering properties enter the problem. At the same time, the nm-sized dust differs from the larger dust in physical properties and interactions are influenced by induced mirror charges.[19] All these processes vary with altitude and from day to night-time and with ionospheric variability. Concerning solar radiation, the photo-ionizing solar X-ray, EUV, and UV fluxes are variable.

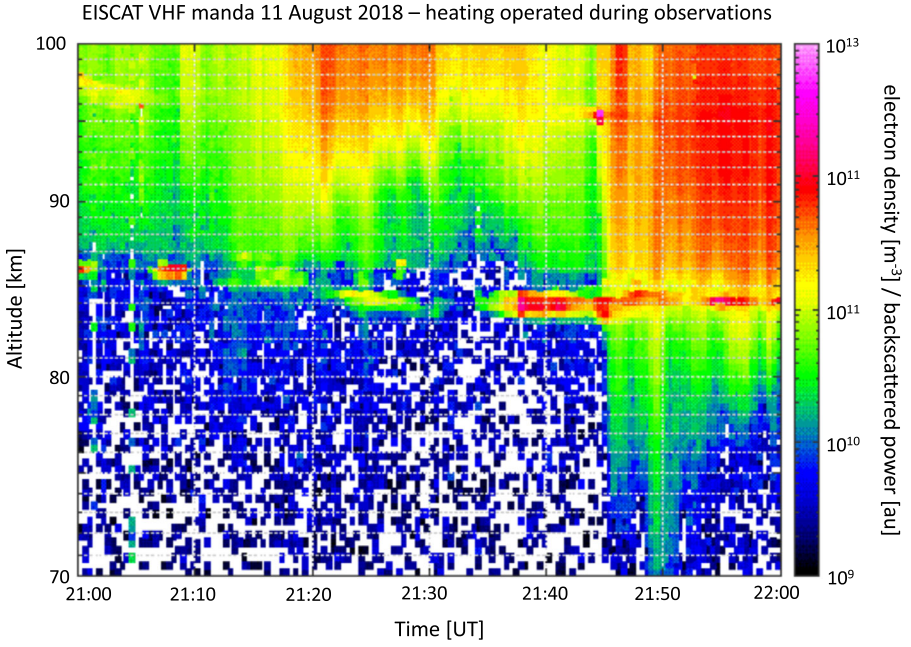

FIGURE 3 Polar Mesospheric Summer Echoes (PMSE) observed with EISCAT VHF radar near Tromsø on August 11, 2018 around local midnight, heating operated during the observation

4 | COHERENT RADAR ECHOES

The charged ice particles contribute to the formation of radar echoes, called Polar Mesospheric Summer Echoes (PMSE),[21–23] which are observed in the polar mesosphere during summer. Height of PMSE is typically 5–20 km and they are at altitude between 70 and 90 km. While the exact formation is still topic of ongoing research, they probably form because of spatial variations in the plasma refractive index. Because the index of refraction at the ω (angular frequency) is $\approx 1 - \omega^2/\omega_p^2$ with $\omega_p \approx (n_e e^2/\varepsilon_0 m_e)^{1/2}$, it is directly influenced by electron density variations. The spatial structures form, because the dust particles are carried in the neutral atmosphere. Full models of the formation of these radar echoes are still missing, but it is assumed that the charging of dust reduces the electron density. Similar radar echoes are observed during the year, but less frequently and at lower altitude,[24] it is suggested that they form in a similar way to PMSE and are linked to smaller dust.[25]

Figure 3 shows PMSE observed from Tromsø on August 11, 2018 during the hour before local midnight from 21:00 to 22:00 UT. Local sunset was 20:11 UT. The small structures around 85 km altitude are PMSE, otherwise the figure displays electron density derived from the observed incoherent back-scattering. The two phenomena can be distinguished by different shape of the frequency spectra. Starting from about 21:45, high electron density is observed as far downward as 70 km. This is typically caused by precipitation of high-energy particles and presumably triggers the PMSE formation because it generates sufficiently high electron densities. Precipitation can, in addition, change the dust charging conditions. This is one of the few observations of PMSE around midnight. During this observation the heating facility[26] was operated, it transmits high-power HF waves into the ionosphere and locally and temporarily enhances the electron temperature. The temperature enhancement at PMSE altitude is by about factor of 10[27] and heating influences the strength of PMSE (cf. ref. [28]). The width of the PMSE frequency spectrum is narrow compared to the incoherent scatter that is discussed below. The spectra shown in Figure 4 are observed with the EISCAT remote receivers that are located at distances 199 km in Kiruna (Sweden) and 391 km in Sodankyla (Finnland) so that the radar echoes are observed under different scattering angles. The spectral profiles are broader than those observed under 180° from Tromsø.[29] We presume that the width is influenced by Doppler-shift due to bulk atmospheric motion along the radar beam, rather than due to the scattering process.[29] While the PMSE shown in Figure 3 have a characteristic wavy pattern in their time evolution and occur at lower altitude, they can also be distinguished from incoherent scatter because they have distinctly different frequency distributions, as shown in Figure 5.

5 | INCOHERENT SCATTER AND CHARGED DUST

The incoherent scatter results from electromagnetic waves scattering off electrons. When the radar wavelength is large in comparison to the plasma Debye length (cf. Figure 1), the spectral distribution of the scattered radiation is influenced by the electron

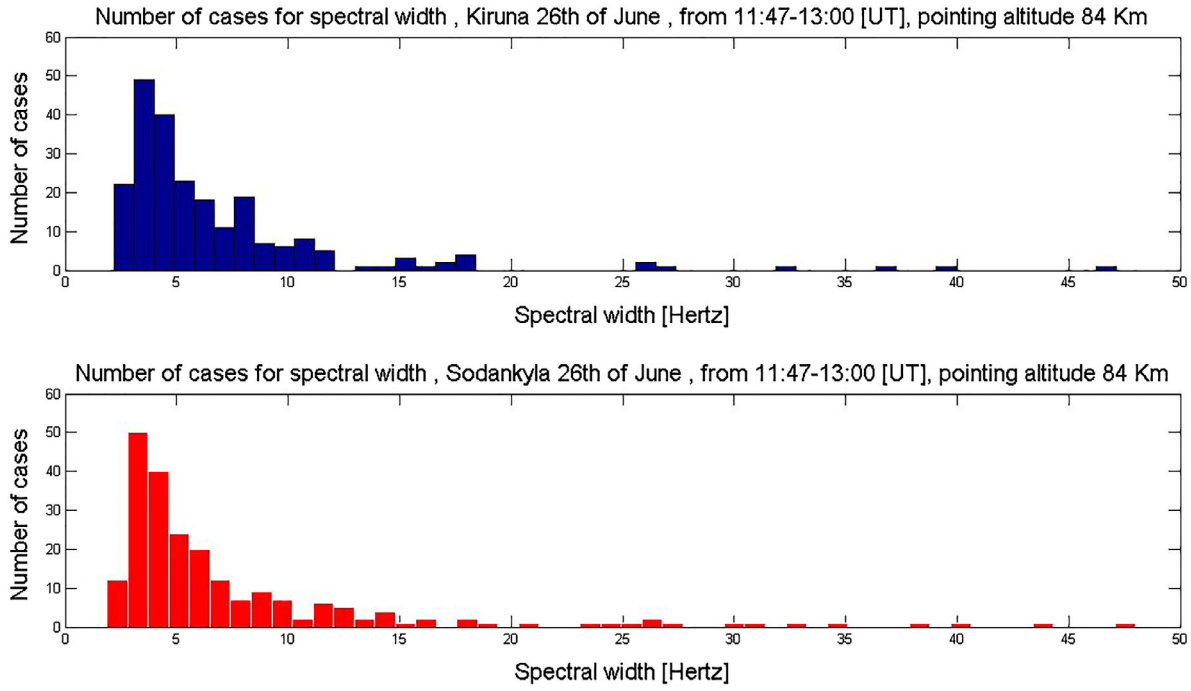

FIGURE 4 The frequency width of Polar Mesospheric Summer Echoes (PMSE) observed on June 26, 2013. The radar signal was transmitted with the EISCAT VHF remote receivers in Sodankylae and Kiruna. The spectra are narrow, in comparison to incoherent scatter but broader than observed in direct back-scattering observed from the Tromsø site

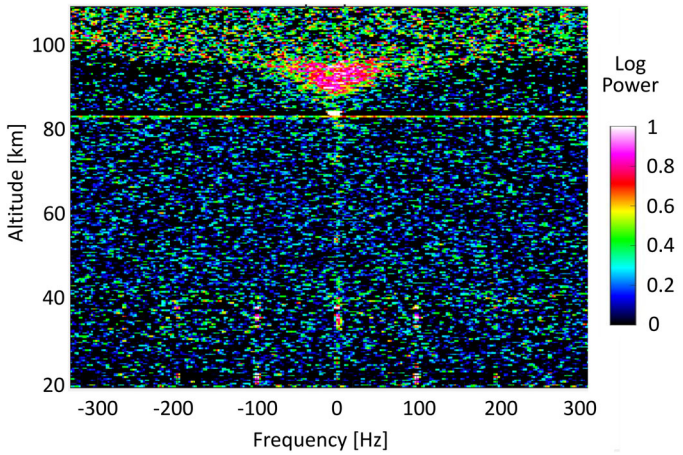

FIGURE 5 A time step of the EISCAT VHF data observed on August 9, 2015 at 22:00 UT. The received back-scattered power relative to maximum received power within this frame is shown with the colour code. The abscissa shows the frequency interval of the received power within ±300 Hz around transmit frequency (set to 0). The ordinate describes the height in the atmosphere from which the signal is scattered, it is derived from the travel time of the signal. The bright spot around 82 km is from Polar Mesospheric Summer Echoes (PMSE). The incoherent scatter ion line above broadens with higher altitude. The horizontal in slightly above 80 km is an artefact

density fluctuations[1] and most apparent are peaks that, in the absence of bulk motion, are shifted upward and downward from the radar transmission frequency by frequencies of the plasma (Langmuir) and by the ion acoustic oscillations of the system. Because of the latter, the vast majority of the observed back-scattered power is concentrated within several 100 Hz around the radar frequency. This usually double-peaked profile, called the ion line, is further influenced by Landau damping so that for $T_i \approx T_e$, which is the case in the lower ionosphere, the resonances smear out and merge to one central peak. Figure 5 shows an example of the ion line and variation with height. The back-scattered power, which, to a large extent, is contained in the ion line is proportional to the electron density. The shape of the ion line depends on electron and ion temperatures, ion mass.

There exist several different theoretical approaches to describe the incoherent scatter. For the lower ionosphere that is weakly ionized and collision dominated, a multi-fluid equation approach is used, e.g., to study the influence of ion components.[30] Cho and collaborators[31] extended results obtained for three fluids to the n-fluid case and included singly charged dust as a constituent. Because we use their incoherent back-scatter radar equation for estimating the spectra observable for EISCAT UHF, we briefly describe it below. For our calculations, we adapted a script described by Theiser.[32] The equation contained in that script differs by a factor π, we used the original radar equation. In the absence of bulk motion and with the

transmit frequency ω_0 of the radar and frequency shifts ω, the multi-fluid model describes the back-scatter radar cross section σ_b by[31]:

$$\sigma_b(\omega_0+\omega)d\omega = \frac{r_e^2 N_e}{\pi\,\omega}\left|\frac{1}{\alpha_e^2 + z_e\left(1+\sum_{s\neq e}\frac{\alpha_s^2}{z_s}\right)}\right|^2 \times\left(\left|1+\sum_{s\neq e}\frac{\alpha_s^2}{z_s}\right|^2 z_e + \frac{\alpha_e^2}{T_e}\sum_{s\neq e}T_s\frac{\alpha_s^2}{z_s^*}\right) \tag{1}$$

with electron number density, N_e, classical electron radius, r_e, and temperatures, T_s, of the atmospheric components. For temperature and other variables used below, the subscript s denotes the constituents ions, electrons, and dust ($s=i$, e, and d). The variables α_s for each constituent are given by:

$$\alpha_s = \frac{1}{k\lambda_{Ds}} = \frac{e}{k}\left(\frac{N_s}{\varepsilon_o k_B T_s}\right)^{1/2}, \tag{2}$$

where λ_{Ds} and N_s are Debye length and number density, respectively, for each component and k is the radar Bragg wave-number, $k=4\pi/\lambda_r$ with the radar wavelength $\lambda_r = c/\omega_0$ where c is the speed of light and ω_0 is the frequency of the radar; k_b is the Boltzmann constant and e is the elementary charge. The variable z_s is given by:

$$z_s = \frac{1+i\frac{5\theta_s}{3\sigma\, s}}{1+i\frac{\theta_s}{\sigma\, s}} + 2i\theta_s\left(\psi_s + \frac{2}{3d_s\psi\, s}\right) - 2\theta_s^2. \tag{3}$$

The variable σ_s (note the subscript) that enters Equation (3) is given as:

$$\sigma_s = \frac{2m_s\psi_s}{m_s+m_n} + \frac{5}{4c_s\psi_s}, \tag{4}$$

where m_s denotes the component mass and ψ_s are the normalized collision frequencies of the electrons, ions, and dust with the neutrals $\psi_s = \nu_{sn}/\sqrt{2}kv_s$, where ν_{sn} are the constituent-neutral collision frequencies described below and $v_s = (k_B T_s/m_s)^{1/2}$ is the mean thermal velocity. The normalized frequencies, θ_s, are given by $\theta_s = \omega/\sqrt{2}kv_s$. Here, m_n is the neutral mass and c_s is the thermal conductivity constant. Finally, the variable β_s is:

$$\beta_s = \frac{2}{3\sigma s} + 2\left[\psi_s + \frac{2}{3d_s\psi_s}\right], \tag{5}$$

where d_s is the viscosity constant. We finally describe the assumed collision frequencies ν_{sn} for the collisions of electron, ion, and dust with the neutrals.

The electron-neutral collision frequency is assumed:

$$\nu_{en} = (3.78\times10^{-11}\;\; T_e^{1/2} + 1.98\times10^{-11}\;\; T_e)N_n. \tag{6}$$

The ion-neutral collisions are assumed:

$$\nu_{sn} = 2.59\times10^{-9}\frac{N_n}{M_s^{1/2}}\sum_t F_t\left(\frac{M_{nt}\;\;\chi_{nt}}{M_s+M_{nt}}\right)^{1/2}, \tag{7}$$

where M_s is the mass of the charged constituent in atomic mass units (amu), F_t is the fractional volume of the neutral gas present, M_{nt} is the mass of each neutral component (in amu), and χ_{nt} is the polarizability of those components.

The dust-neutral collision frequency is assumed:

$$\nu_{sn}^H = \frac{8(r_s+r_n)^2 N_n}{3(m_s+m_n)}\left[\frac{2\pi k_B m_n(m_s T_n + m_n T_s)}{m_s}\right]^{1/2}. \tag{8}$$

This approach (hard-sphere collision) is applicable for dust sizes 0.5 nm and larger. Figure 6 displays the calculated ion line profiles in the presence of charged dust at a frequency of 933 MHz. To calculate the spectrum using Equation (1) for the

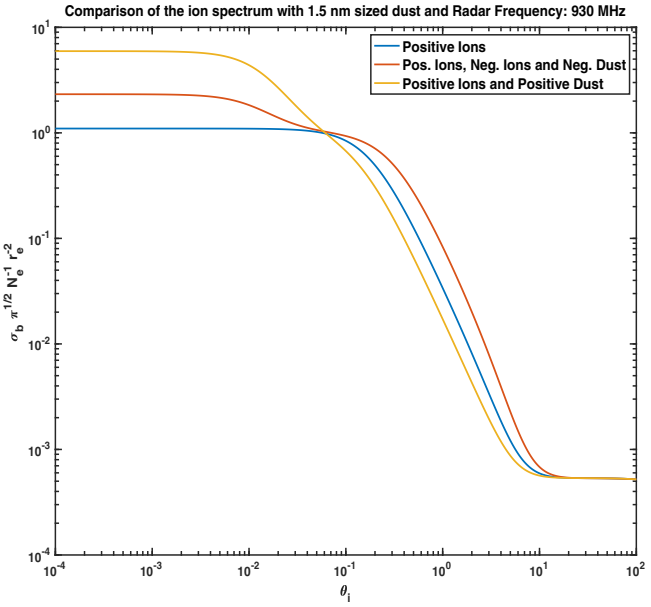

FIGURE 6 Ion line of the radar incoherent scatter spectrum in the presence of 1.5 nm charged dust. Calculations are for 930 MHz radar frequency

radar back-scatter cross section given above, we assume the viscosity constants $d_s = 1.55$, 1.78, 2.1 for electrons, ions, and dust, respectively, and the conductivity constants $c_s = 1.5$, 2.28, and 1.6 given in the same sequence. Following Cho et al., we assume the atmospheric constituents nitrogen, oxygen, argon with volume fractions $M_{N_2} = 0.78$, $M_{O_2} = 0.21$, and $M_{Ar} = 0.1$, and polarizability $\chi_{N_2} = 1.74$, $\chi_{O_2} = 1.57$, and $\chi_{Ar} = 1.64$. For conversion between dust mass and size, we assume spherical compact particles with a mass density of 2 g/cm^3.[5] The dust charge polarity enters through the charge neutrality condition. Figure 6 shows three different ion line spectra. The spectrum without dust is calculated for equal electron and positive ion number densities $N_e = N_i = 5{,}000\,\mathrm{cm}^{-3}$. To calculate the spectrum in the presence of positive dust, we assume $N_e = 5{,}000\,\mathrm{cm}^{-3}$, $N_i = 2{,}500\,\mathrm{cm}^{-3}$, $N_d = 2{,}500\,\mathrm{cm}^{-3}$, and dust radius 1.5 nm. To calculate the spectrum in the presence of negative dust, we assume $N_e = 5{,}000\,\mathrm{cm}^{-3}$, $N_i = 10{,}000\,\mathrm{cm}^{-3}$ for positive ions, $N_i = 2{,}500\,\mathrm{cm}^{-3}$ for negative ions, $N_d = 2{,}500\,\mathrm{cm}^{-3}$, and dust radius 1.5 nm. One can see that the presence of the dust influences the most inner part of the ion line, and that it narrows in the presence of positive dust and widens in the presence of negative dust and positive ions. The model is limited to single charge state, multiples charge states were e.g. studied by Hagfors.[33].

To study the shape of the spectrum, the measured back-scattered power needs to be sufficiently high, which is a challenge for observations in the lower polar ionosphere where electron densities are small and ionospheric variability limits the integration time. The influence of the charged dust on incoherent scatter spectra has been observed only in a few cases so far.[34–36] With the EISCAT radars in northern Scandinavia, so far only one detection of dust signatures in incoherent scatter was reported.[34] This detection was made with the EISCAT 930 MHz near Tromsø during ionospheric conditions with high electron content. A consideration of the dust densities suggests that it is feasible to study the dust signatures in incoherent scatter observed with EISCAT radars. Recent rocket observations from Andøya report dust densities from the 10 cm^{-3} detection limit up to 10,000 cm^{-3}, mostly 100–1,000 cm^{-3},[8] which is of the same order as the densities reported from the few dust detections in incoherent scatter, so far. At mid-latitude, other groups have, in previous studies, derived dust signatures from a long exposure observation with the Arecibo 430 MHz radar. The derived number densities range from 10 to 1,000 cm^{-3} and the dust radii are 0.8–1.0 nm at 85 to 92 km altitude.[34,35] From PFISR 449 MHz observations, the altitude profiles of dust with radii 0.5–2 nm were derived at 70–92 km with 1 hr time resolution close to the Arctic circle (65.1°N, 147.5°W).[36] The EISCAT radars have a nominal transmit power of 2 MW for the UHF radar and 2×1.5 MW for the UHF, which is comparable to the 2 MW of PFISR. Apertures are also comparable, so that we expect it is feasible to detect dust signatures in the spectra. The spectra can be resolved to several 10^{-3} Hz with VHF and to 10^{-3} Hz with UHF and ESR and possibly better for the new EISCAT 3D that is currently under construction.[37,38]

6 | DUST DETECTION IN THE VICINITY OF A METEOR

The present understanding of mesospheric dust is that small solid particles form predominantly by re-condensation from the gas phase. One of the remaining puzzles is that the amounts of metallic ions observed are comparatively small and can be explained with small dust and meteoroid mass flux into the atmosphere.[4] A possible explanation of this observation is that a smaller

fraction of the ablated dust and meteoroid mass is in the gaseous components and that instead more fragments form, possibly also in the nm size range. Fragmentation is observed in a large number of meteors including head echoes.[39] In fact, an observed light curve that showed no apparent signs of fragmentation was recently explained with a model including many small bursts of fragments.[40] The direct formation of nm-sized dust in the fragmentation has not been considered so far.

Let us consider whether dust fragments could be detected directly by its influence on the incoherent scatter spectrum in the vicinity of a meteor. The main part of a meteor forms because the meteoroid surface is heated to evaporation temperature and meteoroid and atmospheric species dissociate and ionize. An expanding column of partially ionized plasma evolves behind the meteoroid and causes the phenomena typically associated with a meteor, called meteor trail. Radio waves are also reflected from the plasma that directly surrounds the meteoroid body and directly moves with it, this phenomenon is called head echo.

The EISCAT VHF radar can observe head echoes with an annual mean rate of 36,600 meteors per day.[41] As a part of the noise reduction, head echoes can be identified in the spectra (and removed). To estimate the probability of detecting incoherent scatter directly from the dust surrounding a meteor, we assume the beam size and empirical meteor flux for VHF radar and note that those will be similar for the new EISCAT 3D operated in an integrated beam mode.[41] The beam cross section at 100 km altitude is 2 km in the east–west direction and 3 km in the north–south direction. For an estimate of the dust number density around the meteor, we assume that a fraction of the meteoroid mass disintegrates in ∼nm particles and that this occurs within 5 km along the beam, a distance that is typical for the ablation of the major mass fraction of the meteoroid.[3] The observed beam volume is sufficiently large to cover the meteor remnants for several minutes. This is most probably long in comparison to the charging time.

A study of the charging of mesospheric dust[42] reports for photoionization of ferric oxide particles with radii 1 nm a time constant of 100 s; it reports shorter time constants for the photo-ionization of larges particles and for the electron attachment. Electron attachment rates increase proportional to the electron density, which is high in the meteor. When considering the conditions in a meteor trail that is formed by a 0.1 g meteoroid, the charging time scale for electron attachment is about 0.5 s at altitude 95 km; the charging time scale is smaller for larger meteors and at lower altitudes.[3] However, because the details of the charging process are still unknown, all these considerations need to be seen with some caution.

In order to reach a detectable average dust density $> 100\,\mathrm{cm}^{-3}$ within this entire volume, the fragmented mass must be $\geq 10^{-2}$ and assuming that the fragments make up 10% of the impacting meteoroid, this would require a 10^{-1} g object, which is at the upper end of the sizes in the meteor head echo population. The interplanetary dust number density and dust flux by number increase steeply to small masses. It is, therefore, plausible to assume that the EISCAT meteor flux, which is a cumulative flux, is dominated by the smallest detectable 10^{-6} g meteoroids. Considering the frequently used interplanetary dust flux model,[43] the cumulative flux at mass 10^{-1} g is a fraction of 10^{-6} of the flux at mass 10^{-6} g, one arrives at one head echo per month (or more) that is caused by a large enough object to influence incoherent scatter at the detection level. This number increases for smaller fragments.

7 | DUSTY PLASMA

Dusty plasma[44] is defined as a plasma that contains charged dust particles that participate in the plasma collective behaviour. In fact, the influence of charged dust on the incoherent scatter and on PMSE can be seen as examples of dusty plasma. But also other dusty plasma phenomena possibly occur. Theory predicts, for instance, that in the presence of negatively charged dust, an ion-acoustic instability builds up and causes Bragg scattering observable with the EISCAT radars.[45] These instabilities formed because of the Bragg condition could be distinguished by a different spectral shape and variation with radar frequency.[21] A frequently used description for dusty plasma condition is that: $a \ll d \ll \lambda_D$,[44] where a is the dust radius, d the average distance between dust particles, and λ_D the plasma Debye length. The dusty plasma condition is often described using the dust number density and introducing the parameter P: $P = 4\pi n_d a \lambda_D^2$, where n_d is the dust number density[46] and for which $P > 1$ describes dusty plasma. When considering this parameter, the difficulties of the dusty plasma description of the ionosphere become apparent. The dust size and number density vary, so that P varies over a broad range and the dusty plasma condition is not always met. In addition, the lower 50–90 km region displays extremely weakly ionized plasma with electron-to-neutral number density ratios of order 10^{-10}, and collisional interactions are often predominant over the electrostatic interactions[1]; electron and ion temperatures are determined by the neutral temperature,[31,33] as well as ion velocity is equal to the neutral wind velocities. The Plasma Debye length that enters the condition ranges from mm to cm, it varies with altitude and from day-time to night-time and conditions are in general highly variable in the polar ionosphere, which makes it an interesting region for observations.

8 | DISCUSSION

The study of charged mesospheric dust with incoherent scatter is an interesting topic, which is feasible, but challenging at present. An advanced radar[37,38] that is under construction at present will improve the measurement capabilities. This can be seen as a motivation to further consider the theory of the electromagnetic wave scattering in the partially ionized medium of the upper atmosphere. The problems, which are analogous to other plasmas, though in a different parameter range include, e.g. the scattering for a size distribution of charged dust particles and in the presence of charge variations. The radar studies of ionospheric dust reveal phenomena that are of interest for understanding dusty plasma. At the same time, the knowledge of the charged dust component is important because of its influence on the physics and chemistry of the ionosphere.

ACKNOWLEDGMENTS

This work was carried out within a project funded by Research Council of Norway, NFR 275503. The EISCAT International Association is supported by research organizations in Norway (NFR), Sweden (VR), Finland (SA), Japan (NIPR and STEL), China (CRIPR), and the United Kingdom (NERC). EISCAT VHF and UHF data are available under http://www.eiscat.se/madrigal/.

ORCID

I. Mann https://orcid.org/0000-0002-2805-3265

REFERENCES

[1] P. Stubbe, T. Hagfors, *Surv. Geophys.* **1997**, *18*, 57.
[2] C. Baumann, M. Rapp, A. Kero, C. F. Enell, *Ann. Geophys.* **2013**, *31*, 2049.
[3] I. Mann, A. Pellinen-Wannberg, E. Murad, O. Popova, N. Meyer-Vernet, M. Rosenberg, T. Mukai, A. Czechowski, S. Mukai, J. Safrankova, Z. Nemecek, *Space Sci. Rev.* **2011**, *161*, 1.
[4] D. A. Mendis, M. Rosenberg, *Chem. Rev.* **2015**, *115*, 4497.
[5] D. M. Hunten, R. P. Turco, O. B. Toon, *J. Atmos. Sci.* **1980**, *37*, 1342.
[6] L. Megner, D. E. Siskind, M. Rapp, J. Gumbel, *J. Geophys. Res.: Atmos.* **2008**, *113*, D3202.
[7] M. Rapp, G. E. Thomas, *J. Atmos. Sol.-Terr. Phys.* **2006**, *71*, 715.
[8] S. Robertson, S. Dickson, M. Horányi, Z. Sternovsky, M. Friedrich, D. Janches, L. Megner, B. Williams, *J. Atmos. Sol.-Terr. Phys.* **2014**, *118*, 161.
[9] J. Hedin, J. Gumbel, T. Waldemarsson, F. Giovane, *Adv. Space Res.* **2007**, *40*, 818.
[10] M. Gadsden, *Space Sci. Rev.* **1982**, *33*, 279.
[11] G. E. Thomas, *Rev. Geophys.* **1991**, *29*, 553.
[12] G. Baumgarten, D. C. Fritts, *J. Geophys. Res.: Atmos.* **2014**, *119*, 9324.
[13] P. Dalin, N. Pertsev, A. Zadorozhny, M. Connors, I. Schofield, I. Shelton, *J. Atmos. Sol.-Terr. Phys.* **2008**, *70*, 1460.
[14] G. Hansen, M. Serwazi, U. von Zahn, *Geophys. Res. Lett.* **1989**, *16*, 1445.
[15] M. E. Hervig, L. E. Deaver, C. G. Bardeen, J. M. Russell, S. M. Bailey, L. L. Gordley, *J. Atmos. Sol.-Terr. Phys.* **2012**, *84*, 1.
[16] J. Gumbel, L. Megner, *J. Atmos. Sol.-Terr. Phys.* **2009**, *71*, 1225.
[17] C. Baumann, M. Rapp, A. Milla, A. Kero, P. T. Verronen, *J. Geophys. Res.* **2015**, *120*, 823.
[18] M. Rapp, I. Strelnikova, B. Strelnikov, P. Hoffmann, M. Friedrich, J. Gumbel, L. Megner, U.-P. Hoppe, S. Robertson, S. Knappmiller, M. Wolff, D. R. Marsh, *J. Geophys. Res.: Atmos.* **2010**, *115*, D00I16.
[19] I. Mann, N. Meyer-Vernet, A. Czechowski, *Phys. Rep.* **2014**, *536*, 1.
[20] M. Rosenberg, R. H. Varney, M. C. Kelley, D. Paschall, *J. Atmos. Sol.-Terr. Phys.* **2012**, *74*, 124.
[21] J. Y. N. Cho, J. Röttger, *Geophys. Res. Lett.* **2012**, *39*, L21102.
[22] M. Rapp, F. J. Lübken, *Atmos. Chem. Phys.* **2004**, *4*, 2601.
[23] C. La Hoz, O. Havnes, L. I. NæSheim, D. L. Hysell, *J. Geophys. Res.: Atmos.* **2006**, *111*, D04203.
[24] R. Latteck, I. Strelnikova, T. Renkwitz, S. Sommer, *EGU General Assembly Conference Abstracts*, **2016**.
[25] O. Havnes, R. Latteck, T. W. Hartquist, T. Antonsen, *Geophys. Res. Lett.* **2018**, *45*, 5727.
[26] M. T. Rietveld, A. Senior, J. Markkanen, A. Westman, *Radio Sci.* **2016**, *51*, 1533.
[27] M. Kassa, M. Rapp, T. W. Hartquist, O. Havnes, *Ann. Geophys.* **2012**, *30*, 433.
[28] A. Senior, A. Mahmoudian, H. Pinedo, C. La Hoz, M. T. Rietveld, W. A. Scales, M. J. Kosch, *Geophys. Res. Lett.* **2014**, *41*, 5347.
[29] I. Mann, N. Meyer-Vernet, A. Czechowski, *J. Geophys. Res.: Space* **2016**, *121*, 11.
[30] J. D. Mathews, *J. Geophys. Res.: Space* **1978**, *83*, 505.
[31] J. Y. N. Cho, M. P. Sulzer, M. C. Kelley, *J. Atmos. Sol.-Terr. Phys.* **1998**, *60*, 349.

[32] G. Teiser, *Diploma Thesis*, Leibniz-Institute of Atmospheric Physics Kuehlungsborn e.V. at the University Rostock, Germany **2013**.
[33] T. Hagfors, *J. Atmos. Sol.-Terr. Phys.* **1992**, *54*, 333.
[34] M. Rapp, I. Strelnikova, J. Gumbel, *Adv. Space Res.* **2007**, *40*, 809.
[35] I. Strelnikova, M. Rapp, S. Raizada, M. Sulzer, *Geophys. Res. Lett.* **2007**, *34*, L15815.
[36] J. T. Fentzke, V. Hsu, C. G. M. Brum, I. Strelnikova, M. Rapp, M. Nicolls, *J. Geophys. Res.* **1997**, *102*, 2001.
[37] U. G. Wannberg, *Radio Sci. Bull.* **2010**, *332*, 75.
[38] I. McCrea, A. Aikio, L. Alfonsi, E. Belova, S. Buchert, M. Clilverd, N. Engler, B. Gustavsson, C. Heinselman, J. Kero, M. Kosch, H. Lamy, T. Leyser, Y. Ogawa, K. Oksavik, A. Pellinen-Wannberg, F. Pitout, M. Rapp, I. Stanislawska, J. Vierinen, *Progress Earth Plan. Sci.* **2015**, *2*, 21.
[39] A. Malhotra, J. D. Mathews, *Geophys. Res. Lett.* **2009**, *36*, L21106.
[40] M. D. Campbell-Brown, R. Blaauw, A. Kingery, *Icarus* **2016**, *277*, 141.
[41] A. Pellinen-Wannberg, J. Kero, I. Häggström, I. Mann, A. Tjulin, *Planet. Space Sci.* **2016**, *123*, 33.
[42] M. Rapp, *Ann. Geophys.* **2009**, *27*, 2417.
[43] E. Grün, H. A. Zook, H. Fechtig, R. H. Giese, *Icarus* **1985**, *62*, 244.
[44] D. A. Mendis, M. Rosenberg, *Ann. Rev. Astron. Astrophys.* **1994**, *32*, 419.
[45] M. Rosenberg, R. L. Merlino, *Planet. Space Sci.* **2007**, *55*, 1464.
[46] O. Havnes, G. E. Morfill, C. K. Goertz, *J. Geophys. Res.* **1984**, *89*, 10999.

How to cite this article: Mann I, Gunnarsdottir T, Häggström I, et al. Radar studies of ionospheric dusty plasma phenomena. *Contributions to Plasma Physics*. 2019;59:e201900005. https://doi.org/10.1002/ctpp.201900005